



ORIGINAL PAPER

**MECHANICAL BEHAVIOR AND CONSTITUTIVE MODEL
OF LOADED COAL WITH CAVITIES****Guangbo CHEN^{1,2)}, Wei TANG¹⁾, Tan LI¹⁾*, Junwen ZHANG³⁾*, Eryu WANG¹⁾,
Chuangye WANG¹⁾, Yejiào LIU¹⁾ and Guohua ZHANG⁴⁾**¹⁾ School of Mining and Coal, Inner Mongolia University of Science and Technology, Baotou 014010, China;²⁾ College of Energy and Mining Engineering, Shandong University of Science and Technology, Qingdao 266590, China;³⁾ School of Energy and Mining, China University of Mining and Technology -Beijing, Beijing 100083, China;⁴⁾ Heilongjiang University of Science and Technology, Harbin 150022, China*Corresponding author's e-mail: litan597@163.com; cgb150617@163.com**ARTICLE INFO****Article history:**

Received 29 August 2025

Accepted 11 November 2025

Available online 27 November 2025

Keywords:Cavity coal sample
Mechanical properties
Acoustical properties
Crack evolution
Constitutive equation
Energy migration**ABSTRACT**

Cavity-like defects in coal-rock masses are highly likely to cause local or overall damage, and may even trigger dynamic disasters such as roadway collapse and rockburst. To gain a deeper understanding of how cavities affect the mechanical properties and failure behavior of coal, axial compression numerical experiments were conducted on coal samples with five different cavity radii and five different cavity shapes. The result shows that: 1) With the increase of cavity radius, the compressive strength, elastic modulus, pre-peak strain energy, impact energy index continuously decreases, with the deterioration degree of compressive strength being 0.6 %, 9.5 %, 119.2 %, and 24.8 % respectively. 2) The cavity shape has little effect on the compressive strength, impact energy index. The triangular prism cavity has the greatest influence on elastic modulus, while the cylindrical cavity has the least influence on the elastic modulus. The pre-peak strain energy of cylindrical cavity coal sample is the largest, while the pre-peak strain energy of triangular prism cavity coal sample is the smallest. 3) As the cavity radius increases, the peak ringing count, the crack initiation stress and the cumulative ringing count gradually decrease. The cavity shape has little effect on the cumulative ringing count. 4) The larger the cavity radius, the greater the influence on the crack. As the cavity radius increases, the crack initiates gradually near the cavity and dominates the failure of the sample. 5) Based on the statistical distribution theory and the D-P strength criterion, the damage constitutive equation of the cavity coal sample is constructed and the rationality is verified. 6) The energy migration model of instability and failure of coal samples with cavities was constructed. The energy accumulation, migration and release of coal samples with cavities under loaded conditions were analyzed, and the instability mechanism of coal samples with cavities was clarified. The research has important theoretical guiding significance for roadway support design, mining engineering stability evaluation and coal-rock geological dynamic disaster prevention and control.

1. INTRODUCTION

Nowadays, shallow easy-to-mine coal resources in our country have been exhausted, and coal resources development have gradually entered the deep mining stage (Qi et al., 2020; Pan et al., 2021; Yuan, 2021). As the depth of mining increases, the frequency and intensity of coal-rock dynamic disasters have increased significantly, posing a serious threat to the safe production of coal mines and the safety of personnel.

The essence of coal-rock dynamic disaster is that a large amount of elastic energy accumulated in coal is released rapidly under the influence of disturbance, which leads to the instantaneous instability of coal-rock system. As a natural material, coal is rich in a large number of internal cavities due to formation conditions, tectonic movements, weathering and stripping. The greater the mining depth, the more cavities there are in the coal body. Under the action of mine pressure, these cavities are squeezed and deformed to generate new cracks. The new cracks are

connected with the original cracks in the coal body, resulting in the deterioration of the local or overall mechanical properties of the coal body, which in turn leads to the instability and failure of the coal-rock system, causing coal-rock dynamic disasters such as collapse and impact.

The cavity has an important influence on the mechanical properties and failure mechanism of coal and rock. Many scholars have carried out a lot of research work and achieved fruitful results. Zhang et al. (2021) studied the mechanical properties of gypsum samples with cavities under different loading rates, the evolution characteristics of cracks around cavities, and revealed the mechanism of loading rate effect. Lai et al. (2021a, 2021b) studied the failure characteristics and energy evolution law of coal samples with different cavity radii from the perspective of borecavity pressure relief to prevent rock burst. Xiao et al. (2022) studied the influence of cavity radius on the mechanical properties, failure characteristics and energy migration of coal samples,

and analyzed the changes of acoustic emission characteristics during loading. Wu et al. (2023) studied the dynamic characteristics and failure mechanism of vuggy sandstone in combination with the common roadway section shape in engineering. Wang et al. (2023) studied the effects of cavity radius on the strength, deformation, and energy of the specimens, as well as the characteristics of crack propagation by conducting Hopkinson bar impact tests on sandstone specimens containing cavities. Gong et al. (2023) analyzed the dynamic compressive strength, dynamic modulus of deformation, failure modes, and crack propagation behavior by conducting Hopkinson bar impact tests on limestone specimens containing double cavities and flaws. Li et al. (2015) investigated the mechanical failure characteristics and crack propagation characteristics of specimens under impact load by conducting Hopkinson bar impact tests on marble specimens containing cavities. Zhou et al. (2021) investigated the strain evolution laws and failure characteristics of rock with different numbers and arrangements of cavities by conducting drop-weight impact tests on granite samples containing cavities. Yang et al. (2012) studied the strength, deformation, acoustic emission, and crack propagation characteristics of sandstone containing cavities and fractures by conducting uniaxial compression tests. Zhao et al. (2019) conducted uniaxial compression tests on red sandstone samples containing cavities to analyze the deformation and fracturing evolution of samples, as well as the impact of cavity shape on the mechanical properties and the evolution of fracturing and damage. Ge et al. (2022) and Wang et al. (2022) analyzed the influence of asymmetric load on the deformation and damage law of raw coal and briquette with central cavities, and established a damage constitutive model. Wang et al. (2024) studied the crack propagation, failure mode and fractal characteristics of composite rock (soft and hard rock) with prefabricated cracks and cavities under uniaxial compression by using RFPA^{2D} simulation. Liu (2022) quantitatively studied the mechanical properties and fracture behavior of rock-like specimens with cavities and cracks. Huang et al. (2023) studied the peak strength, elastic modulus, acoustic emission characteristics and crack propagation characteristics of red sandstone samples with cavity-crack defects by using particle flow code PFC^{2D}. Liu et al. (2024) revealed the influence of cavity shape on the mechanical properties and failure modes of layered rocks by using the finite element-discrete element coupled numerical simulation method (FDEM). Liu et al. (2023) studied the mechanical properties and acoustic emission characteristics under eccentric load by carrying out eccentric load tests on three-cavity sandstone with different morphologies. Pi et al. (2023) carried out a numerical simulation study on the fracture process of sandstone with D-shaped cavities under biaxial loading and unloading conditions, and studied its mechanical properties and crack propagation characteristics. Zhao et al. (2023) studied the mechanical properties and fracture characteristics

of cylindrical cavity granite under one-dimensional dynamic and static combined loading. Li et al. (2022) carried out experimental research on the influence of stress wave disturbance on the ultra-low friction effect of sandstone block with cavities, and analyzed the corresponding energy variation characteristics of the working block under different working conditions.

From the above research, it can be seen that the research on the influence of cavities on the mechanical properties of rock mainly focuses on rock samples such as sandstone, limestone, marble, granite, red sandstone and gypsum samples, but there are few reports on coal samples. The reason is that it is particularly difficult to prepare coal samples with cavities due to the fact that coal is a soft rock material. In addition, the mechanical properties of the sample are easily affected by the preparation process like cutting or grinding. The development of numerical simulation technology effectively makes up for this defect, which can not only test the mechanical properties of coal samples with cavities, but also reproduce the evolution process of cracks well. It has become an important means to study the mechanical properties of rock.

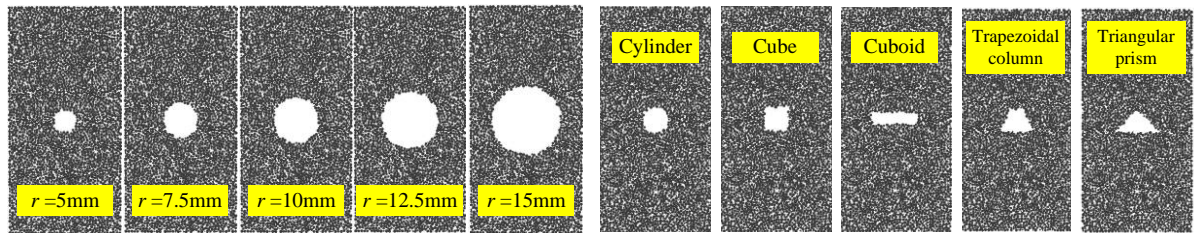
Based on this, the axial compression numerical tests were carried out on coal samples with different cavity radii and cavity shapes. The effects of cavity radius and cavity shape on mechanical properties, acoustic emission characteristics and impact effects were studied. The crack evolution characteristics of coal samples under the influence of cavity radius and cavity shape were analyzed. The instability model of coal containing cavities was constructed, and the internal energy migration law of coal containing cavities was analyzed. The damage constitutive equation was established and verified, and the instability and failure mechanism of energy migration of coal containing cavities was revealed, in order to provide a useful reference for roadway support design, stability evaluation of coal-rock system and prevention and control of coal-rock geological dynamic disasters.

2. NUMERICAL TEST OF AXIAL COMPRESSION OF COAL SAMPLES WITH CAVITIES

Based on the structure of coal-rock, numerical simulation-based mechanical testing of cavity-containing coal bodies is the main research method employed in this paper. In the early stage of planning, we intended to prepare physical cavity-containing coal samples for mutual verification of theoretical and experimental results. However, this approach proved extremely challenging: the sample preparation process is highly susceptible to vibrations from coring machines, cutting machines, and grinding machines, which cause irreversible mechanical damage to the internal structure of the samples. Additionally, creating cavities in intact coal samples is even more difficult with an extremely low success rate. Even if porous coal samples are successfully prepared, their mechanical properties deviate significantly from actual engineering conditions due to multiple damages

Table 1 The values of the microscopic parameters.

Parameter	Value	Parameter	Value
Model height/mm	100	Maximum particle radius / mm	0.8
Model radius / mm	50	Particle friction factor	0.5
Porosity	0.15	Particle density / kg·m ⁻³	2000
Minimum particle radius / mm	0.6	Tensile strength / MPa	7
Internal friction angle / °	30	Cohesion / MPa	4
Stiffness ratio	1.5	Contact modulus / GPa	1.5

**Fig. 1** Cross section of numerical model of coal samples with cavities.

during preparation, rendering the research results under such conditions of limited value. Considering the aforementioned preliminary research challenges and sample preparation constraints, we adopted the numerical simulation method to study the mechanical properties and instability mechanism of cavity-containing coal samples. The mechanical parameters of coal samples in the numerical simulation are based on laboratory-measured mechanical data, ensuring that the simulation results align with actual engineering scenarios.

2.1. CONSTRUCTION OF COAL SAMPLE MODEL WITH CAVITIES

The axial compression test of coal samples with cavities was carried out by PFC numerical simulation software. The particles of the coal sample with cavities were in linear parallel bonding contact, and a cylindrical model with a radius of $\varphi 50 \text{ mm} \times 100 \text{ mm}$ was generated in PFC, and then Balls with different radius radii were generated by using random seed 10001 in this area. The minimum particle radius was 0.06 mm and the maximum particle radius was 0.08 mm. The density was set at 2000 kg/m³. The damping coefficient between the particles and the wall was set to 0.7. The values of the microscopic parameters of the model are shown in Table 1.

In order to study the mechanical properties and crack evolution law of coal samples with different cavity radii and cavity shapes, 10 kinds of coal samples with cavities were designed: (1) Coal samples with different cavity radii: the radius of the cavity is 5 mm, 7.5 mm, 10 mm, 12.5 mm, 15 mm, respectively, numbered S-1, S-2, S-3, S-4, S-5. Figure 1(a) is the vertical section along the center of the coal body. (2) Coal samples with different cavity shapes: cylinder, cube, cuboid, trapezoidal column, triangular prism, numbered P-1, P-2, P-3, P-4, P-5 in turn, which have

the same volume in five kinds cavity. Figure 1(b) is the vertical section along the center of the coal body.

2.2. TEST SCHEME AND TEST RESULTS

In order to obtain the complete stress-strain curve of the sample, the static displacement loading method was selected to carry out the uniaxial compression test on the sample at a loading rate of 0.005 mm/s.

The mechanical parameter data (Table 2) of the coal samples with cavities were obtained by the test.

3. ANALYSIS OF MECHANICAL PROPERTIES OF COAL SAMPLES WITH CAVITIES

According to the mechanical data in Table 2, the mechanical properties evolution curves of coal samples with different cavity radii and cavity shapes is shown in Figure 2. According to Figure 2, the compressive strength, elastic modulus, pre-peak strain energy and impact energy index are analyzed one by one.

3.1. EFFECT OF CAVITIES ON COMPRESSIVE STRENGTH OF COAL SAMPLES

It can be seen from Figure 2(a) that the cavity radius has a significant effect on the compressive strength of the samples. The compressive strength of S-1 coal sample is the largest, which is 17.09 MPa, and the compressive strength of S-5 coal sample is the smallest, which is 9.32 MPa. It can be seen that with the increase of cavity radius, the compressive strength of the sample decreases continuously. The deterioration degree is defined as the ratio of the reduction of a mechanical parameter (e.g., compressive strength) from its initial value to the initial value, expressed as a percentage. It serves as a quantitative indicator to characterize the extent to which a mechanical parameter decreases from its initial state, reflecting the attenuation degree of the

Table 2 Numerical simulation results of different cavity radii.

Number	Compressive strength /MPa	Peak strain /MPa	Elastic module /MPa	Pre-peak elastic strain energy/kJ	Impact energy index K_E
S-1	17.09	0.51	3725.9	0.0492	7.45
S-2	16.95	0.48	3643.6	0.0428	6.90
S-3	15.35	0.41	3551.2	0.0313	3.96
S-4	12.40	0.34	3399.2	0.0197	2.05
S-5	9.32	0.32	2681.2	0.0145	2.01
P-1	16.73	0.53	3527.5	0.0473	4.60
P-2	16.48	0.53	3438.9	0.0422	4.40
P-3	16.33	0.54	3399.1	0.0351	4.11
P-4	16.27	0.52	3285.4	0.0284	3.90
P-5	16.10	0.53	3015.8	0.0167	3.51

mechanical parameter under the influence of certain factors. The deterioration degree of compressive strength was calculated to be 0.8 %, 10.2 %, 27.4 % and 45.5 %, respectively. It shows that the influence of cavity radius on compressive strength is non-uniform. The relationship between cavity radius and compressive strength conforms to $y = 15.03 + 0.85x - 0.08x^2$, and the goodness of fit is 0.99. When the cavity radius is 0 ~ 7.5 mm, the compressive strength decreases slightly and the deterioration is slow, which is the slow decrease area of compressive strength. When the cavity radius is 7.5 ~ 15 mm, the compressive strength decreases greatly and the deterioration is fast, which is the sharp drop area of compressive strength.

It can be seen from Figure 2(b) that the cavity shape has a certain influence on the compressive strength of the sample. The compressive strength of P-1 coal sample is the largest, which is 16.73 MPa, and the compressive strength of P-5 coal sample is the smallest, which is 16.10 MPa. In addition, the compressive strength of P-5 coal sample is small. The reason is that the cavity shape of P-5 coal sample is triangular prism. The upper side of triangular prism has a small stress area when loading, which is more likely easy to form stress concentration and damage. The deterioration degrees of compressive strength under the influence of cavity shape were 3.6 %, 4.4 %, 4.8 % and 5.8 %, respectively. It shows that the compressive strength of coal samples under the influence of cavity shape is reduced, but the decline is relatively small.

3.2. EFFECT OF CAVITIES ON ELASTIC MODULES OF COAL SAMPLES

It can be seen from Figure 2(a) that the cavity radius has a significant effect on the elastic modulus of the sample. The elastic modulus of S-1 coal sample is the largest, which is 3725.9 MPa, and the elastic modulus of S-5 coal sample is the smallest, which is 2681.2 MPa. It can be seen that with the increase of cavity radii, the elastic modulus of the sample decreases continuously. The relationship between cavity radius and elastic modulus conforms to $y = \exp(3698.44, -1.15, -2.21)$, and the goodness of fit is 0.98. When the cavity radius is 5 ~ 12.5 mm, the elastic modulus decreases slightly and the

deterioration is slow, which is the slow drop area of elastic modulus. When the cavity radius is 12.5 ~ 15 mm, the elastic modulus greatly decreases with a deterioration degree of 21.12 %, which is a sharp drop area of elastic modulus.

It can be seen from Figure 2(b) that the influence of cavity shape on the elastic modulus of the sample is obvious. The elastic modulus of P-1 coal sample is the largest, which is 3527.5 MPa, and the compressive strength of P-5 coal sample is the smallest, which is 3015.8 MPa. The elastic modulus of the samples from large to small is P-1, P-2, P-3, P-4, P-5. The triangular prism shaped cavity has the greatest influence on the coal sample, and the cylindrical cavity has the least influence on the coal sample. The deterioration degree of elastic modulus under the influence of cavity shape is calculated, and the deterioration degree of elastic modulus is 4.1 %, 6.5 %, 10.5 % and 29.4 % respectively. It shows that the elastic modulus of coal samples decreases greatly under the influence of cavity shape.

3.3. EFFECT OF CAVITIES ON PRE-PEAK STRAIN ENERGY OF COAL SAMPLES

It can be seen from Figure 2(a) that the cavity radius has a significant effect on the pre-peak strain energy of the sample. The pre-peak strain energy of S-1 coal sample is the most, which is 0.0492 kJ, and the pre-peak strain energy of S-5 coal sample is the least, which is 0.0145 kJ. It can be seen that with the increase of cavity radius, the pre-peak strain energy of the sample decreases continuously. The cavity radius has a linear relationship with the pre-peak strain energy, and the relationship between the cavity radius and the pre-peak strain energy conforms to $y = 0.0685 - 0.0037x$, and the goodness of fit is 0.98.

It can be seen from Figure 2(b) that the cavity shape also has a certain influence on the pre-peak strain energy of the sample. The pre-peak strain energy of P-1 coal sample is the most, which is 0.0473 kJ, and the pre-peak strain energy of P-5 coal sample is the least, which is 0.0167 kJ. In addition, the pre-peak strain energy of P-5 coal sample is small. The reason is that the cavity shape of P-5 coal sample is triangular prism. The stress area on the upper side of the triangular prism is small under the load condition,

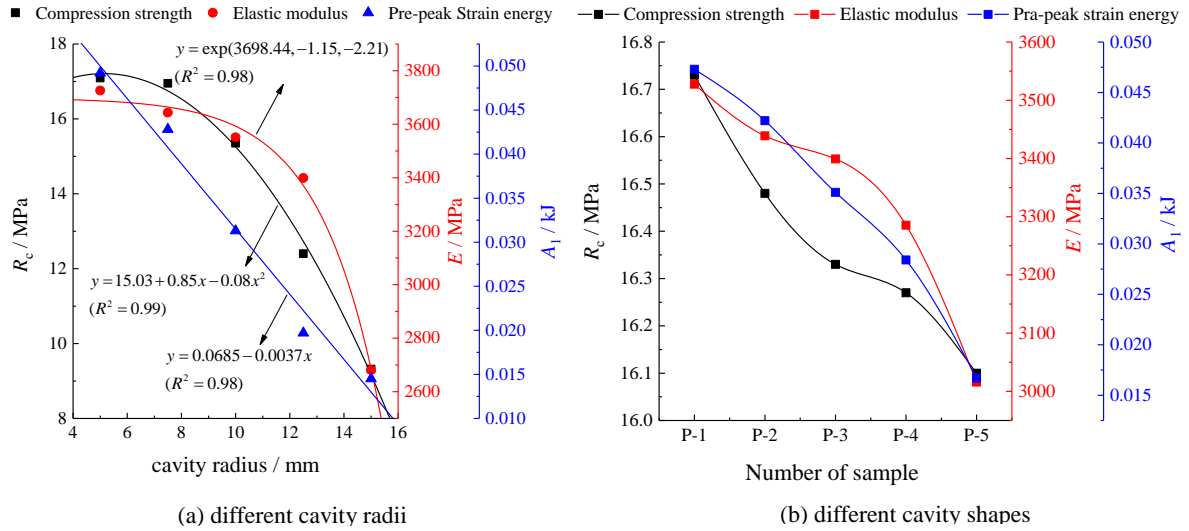


Fig. 2 Evolution law of mechanical properties of coal samples with cavities.

which is easy to form stress concentration and damage, and not easy to accumulate energy.

3.4. EFFECT OF CAVITIES ON IMPACT ENERGY INDEX OF COAL SAMPLES

The impact tendency of coal is a core indicator for assessing the risk of rock burst disasters, characterizing the inherent property of coal to accumulate deformation energy and undergo burst failure under mining-induced stress. The impact energy index K_E is one of the key indicators for evaluating the impact tendency of coal, reflecting the capacity of coal to release burst energy during failure. A higher value of K_E indicates a stronger impact tendency of the coal. The impact energy index is commonly used to assess the impact tendency of coal and rock, which is classified into three grades: none, weak, and strong. Specifically, the impact energy index refers to the ratio of the deformation energy accumulated before the peak of the stress-strain curve of a coal sample under uniaxial compression to the deformation energy consumed after the peak. This index can intuitively and comprehensively reflect the entire process of energy accumulation and consumption, revealing the physical essence of impact tendency. The classification criteria are as follows: $0 < K_E < 1.5$ indicates no impact tendency; $1.5 \leq K_E < 5.0$ indicates a weak impact tendency; and $K_E \geq 5.0$ indicates a strong impact tendency. It can be seen from Figure 3 that the impact energy index of coal samples is more significantly affected by the cavity radius. As the cavity radius increases, the impact energy index of coal samples gradually decreases. The impact energy index of coal samples with five cavity radii ranges from 2.01 to 7.45, which varies greatly. The impact energy indexes of S-1 coal sample with cavity radius of 5 mm and S-2 coal sample with cavity radius of 7.5 mm are 7.45 and 6.9, respectively, both of which are strong impact tendency. The impact energy index of S-3, S-4 and S-5 samples are 3.96, 2.05 and 2.01, respectively, all of

which are weak impact tendency. In addition, it is found that the cavity shape has little effect on the impact energy index of coal samples. The impact energy index of the five cavity-shaped coal samples ranges from 4.60 to 3.51, all of which are weak impact proneness.

4. ACOUSTIC CHARACTERISTICS ANALYSIS OF COAL SAMPLES WITH CAVITIES

Acoustic emission can directly reflect the evolution law of internal damage of rock. The ringing count refers to the number of oscillations of the acoustic emission signal crossing the threshold voltage, which reflects the acoustic emission signal intensity and frequency of coal-rock mass. It is widely used for the evaluation of acoustic emission activities and the quantitative evaluation of coal and rock damage. In numerical simulation, every time a particle bond is broken, it is regarded as one ringing.

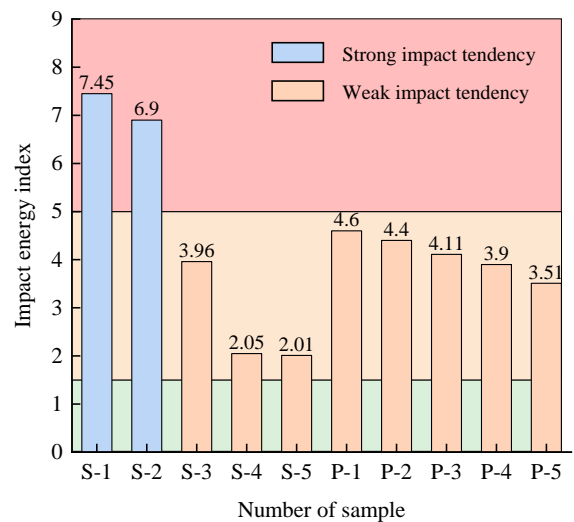


Fig. 3 Impact energy index of coal samples with cavities.

4.1. ACOUSTIC EMISSION ANALYSIS OF COAL SAMPLES WITH DIFFERENT CAVITY RADII

Figure 4 is the stress-strain-impact number curve of coal samples with different cavity radii. From Figure 5, it can be seen that:

- (1) Peak ringing count. There is a significant difference in the peak ringing counts of coal samples with different cavity radii. The peak ringing count of S-1 coal sample, S-2 coal sample, S-3 coal sample, S-4 coal sample, S-5 coal sample are 10109 times, 14061 times, 8407 times, 4658 times, 2293 times, respectively. The order of peak ringing count is: S-2 coal sample > S-1 coal sample > S-3 coal sample > S-4 coal sample > S-5 coal sample. It shows that with the increase of cavity radius, the peak ringing count shows a downward trend, and the larger the cavity radius, the more obvious the decline.
- (2) Initiation stress. There is a difference in the initiation stress of coal samples with different cavity radii as well. The S-1 coal sample and the S-2 coal sample both began to develop cracks at a strain around of 0.3 %, with similar initiation stress, which are approximately 10 MPa and 9.89 MPa, respectively. S-3 coal sample began to develop cracks at a strain of 0.21 %, with the initiation stress of 6.56 MPa. The coal sample of S-4 began to develop cracks at a strain of 0.18 %, with the initiation stress of 5.67 MPa. The S-5 coal sample began to develop cracks at a strain of 0.14 %, with the initiation stress of 3.99 MPa. It can be seen that as the radius of the cavity increases, the initiation stress gradually decreases.
- (3) Cumulative ringing count. Cumulative ringing count. The S-2 coal sample with a cavity radius of 7.5 mm has the highest cumulative ringing count, which is 2,261,404 times. The cumulative ringing counts of S-1, S-3, S-4, and S-5 coal samples are 2,228,714 times, 1,724,403 times, 1,344,562 times, and 950,130 times respectively. It can be seen that with the cavity radius increases, the cumulative ringing count gradually decreases, which is negatively correlated with the cavity radius. The cumulative ringing counts are shown in Figure 5. The cumulative ringing count of S-1 coal sample with a cavity radius of 5 mm and S-2 coal sample with a cavity radius of 7.5 mm are not much different, and the degree of cracks in the two specimens is similar. The cumulative ringing count decreased from 7.5 mm to 10 mm, and the deterioration degree was 23.7 %. The cumulative ringing count decreased from 10 mm to 12.5 mm, and the deterioration degree was 22 %. The cumulative ringing count decreased from 12.5 mm to 15 mm with the deterioration degree of 29.3 %, which had the highest deterioration degree of this stage. When the cavity radius is more than 7.5 mm, the damage degree of the specimen has changed obviously. What's more, when the cavity radius is more than 12.5 mm, the coal sample is seriously damaged.

4.2. ACOUSTIC EMISSION ANALYSIS OF COAL SAMPLES WITH DIFFERENT CAVITY SHAPES

Figure 6 is the stress-strain-impact times curve of coal samples with different cavity shapes. From Figure 6, it can be seen that:

- (1) Peak ringing count. There is a significant difference in the peak ringing count among coal samples with different cavity shapes. The peak ringing count for the P-1 coal sample, P-2 coal sample, P-3 coal sample, P-4 coal sample, P-5 coal sample are 11,282 times, 11,124 times, 14,447 times, 12,503 times, 16,178 times, respectively. The ranking of peak ringing count is: P-5 sample > P-3 sample > P-4 sample > P-1 sample > P-2 sample.
- (2) Initiation stress. There are differences in the initiation stress among coal samples with different cavity shapes. The P-1 coal sample with cylindrical cavity began to develop cracks at a strain of 0.26 %, and the initiation stress was 8.34 MPa. The P-2 coal sample of the cube cavity began to develop cracks at a strain of 0.25 %, and the initiation stress was 8.36 MPa. The P-3 coal sample of the cuboid cavity began to develop cracks at a strain of 0.26 %, and the initiation stress was 8.52 MPa. The P-4 coal sample of the trapezoidal column cavity began to develop cracks at a strain of 0.22 %, and the crack initiation stress was 7.05 MPa. The P-5 coal sample of the triangular prism cavity began to develop cracks at a strain of 0.21 % with the crack initiation stress of 6.81 MPa, which had the smallest initiation stress of the coal sample. And the initiation strain of the remaining coal samples is roughly distributed near 0.26 %.
- (3) Cumulative ringing count. There is no obvious law in the cumulative ringing count of the five coal samples. The triangular prism cavity P-5 coal sample has the highest cumulative ringing count at 2,274,840 times, while the cylindrical cavity P-1 coal sample has the lowest impact count at 2,164,493 times, with a difference of only 4.8 % between the two. This shows that the internal damage degree of the five coal samples is roughly the same. Additionally, the compressive strengths of the five coal samples do not differ significantly, which also corroborates the law of cumulative acoustic emission impact times.

5. CRACK EVOLUTION LAW OF COAL SAMPLES WITH CAVITIES

5.1. CRACK EVOLUTION LAW OF COAL SAMPLES WITH DIFFERENT CAVITY RADII

In the numerical model, when the contact force between particles is greater than the set bond strength, the bond between particles will break, resulting in the generation of cracks. The left part of Figure 7 shows the crack propagation process in coal samples with different cavity radii, and the right part shows the evolution of bond breakage in the profile of coal samples with different cavity radii.

For the S-1 coal sample with a cavity radius of 5 mm, cracks first appeared around the cavity. As the loading continues, fine cracks began to appear below

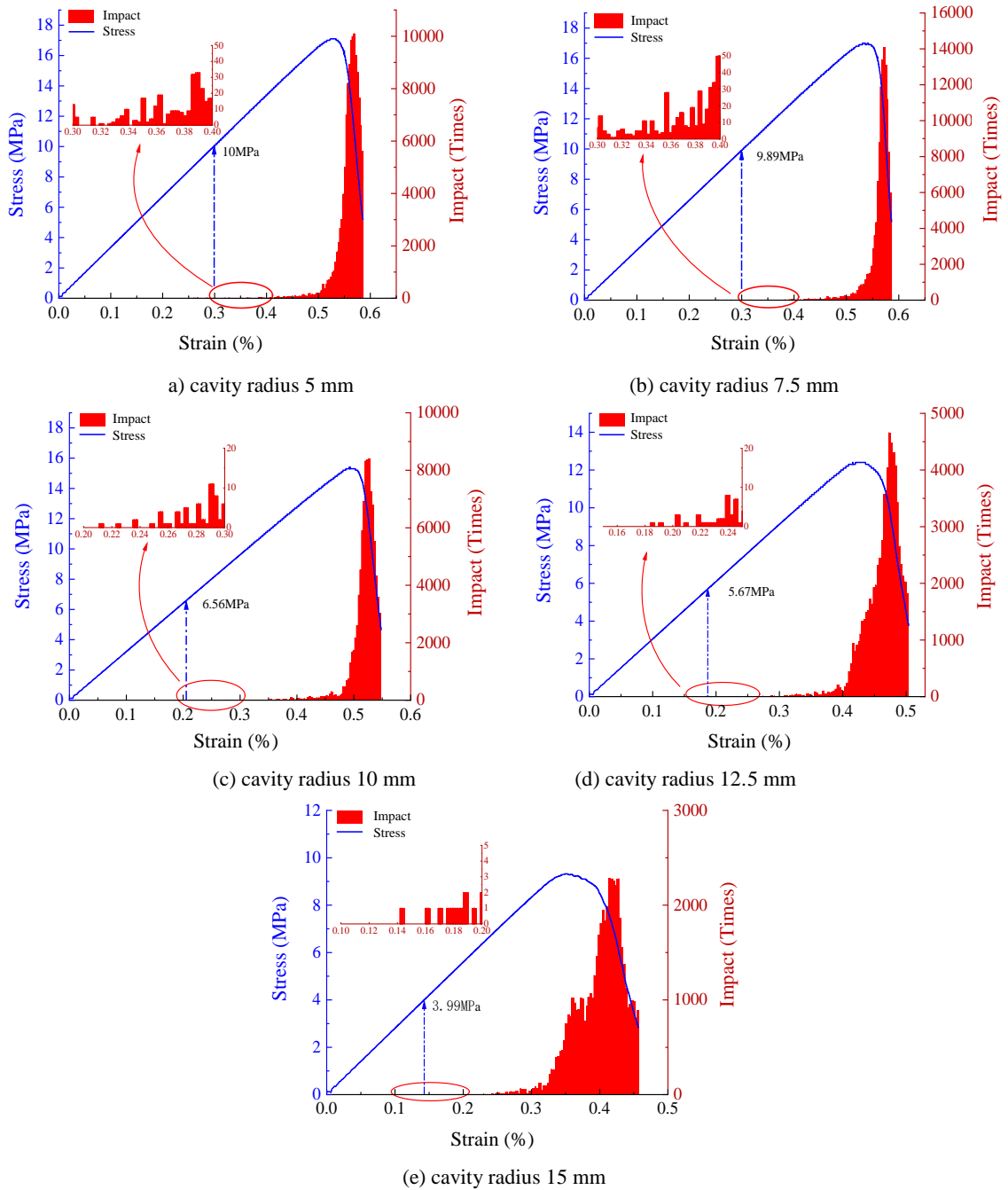


Fig. 4 Images of stress-strain-impact times of coal samples with different cavity radii.

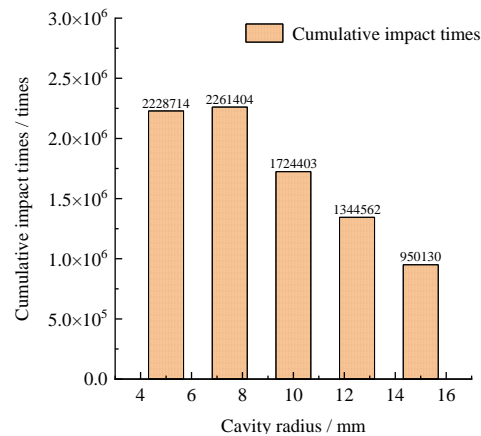


Fig. 5 Image of cavity radius and cumulative ringing count.

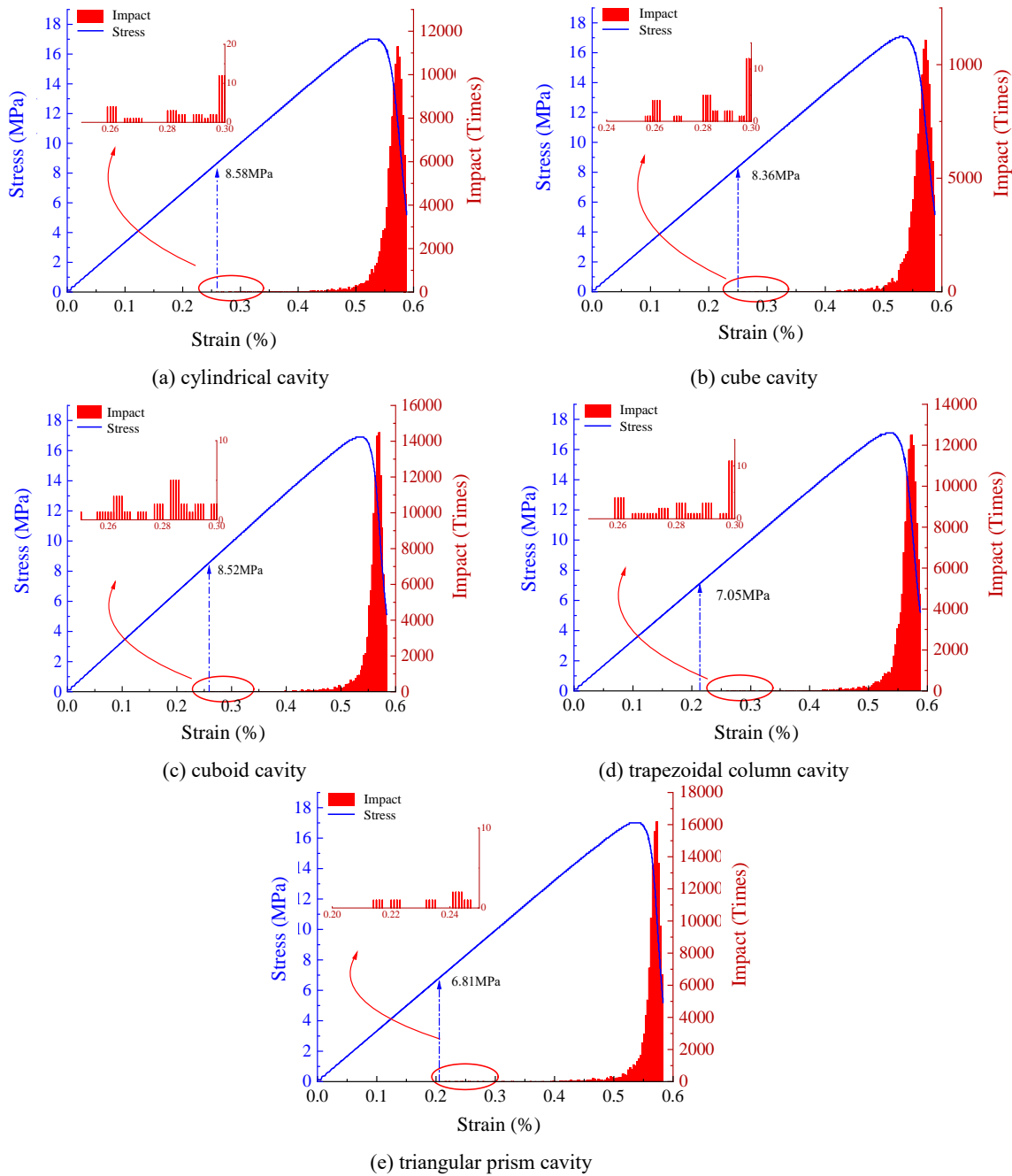


Fig. 6 Stress-strain-impact times curves of coal samples with different cavity shapes.

the cavity. The failure mainly occurs at the lower end surface of the specimen, and the influence of the cavity on the failure mode of the specimen is not obvious.

For the S-2 coal sample with a cavity radius of 7.5 mm, there are many cracks in the lower part of the specimen. Cracks first germinated at the lower left of the cavity. As the loading continues, cracks also appeared at the upper right of the cavity. Eventually, a shear band that runs from the lower left to the upper right was formed. Meanwhile, a similar parallel shear band and diffuse cracks were generated below this shear band. In general, the failure of the sample is mainly concentrated in the lower half of the sample, and the cavity has a relatively small impact on the failure of the specimen.

For the S-3 coal sample with a cavity radius of 10 mm, the cavity has a certain influence on the failure of the specimen. Cracks were generated simultaneously at the lower left and upper right of the cavity. The width of the shear band was greater than that of the shear bands of S-1 and S-2 coal samples. And a group of cracks were also generated in the upper and lower directions of the cavity. These two groups of cracks developed in one group horizontally and one group vertically. The horizontally developed cracks were more significant and played a major role in the failure of the sample.

For the S-4 coal sample with a cavity radius of 12.5 mm, an obvious stress concentration area was formed around the cavity during the compression

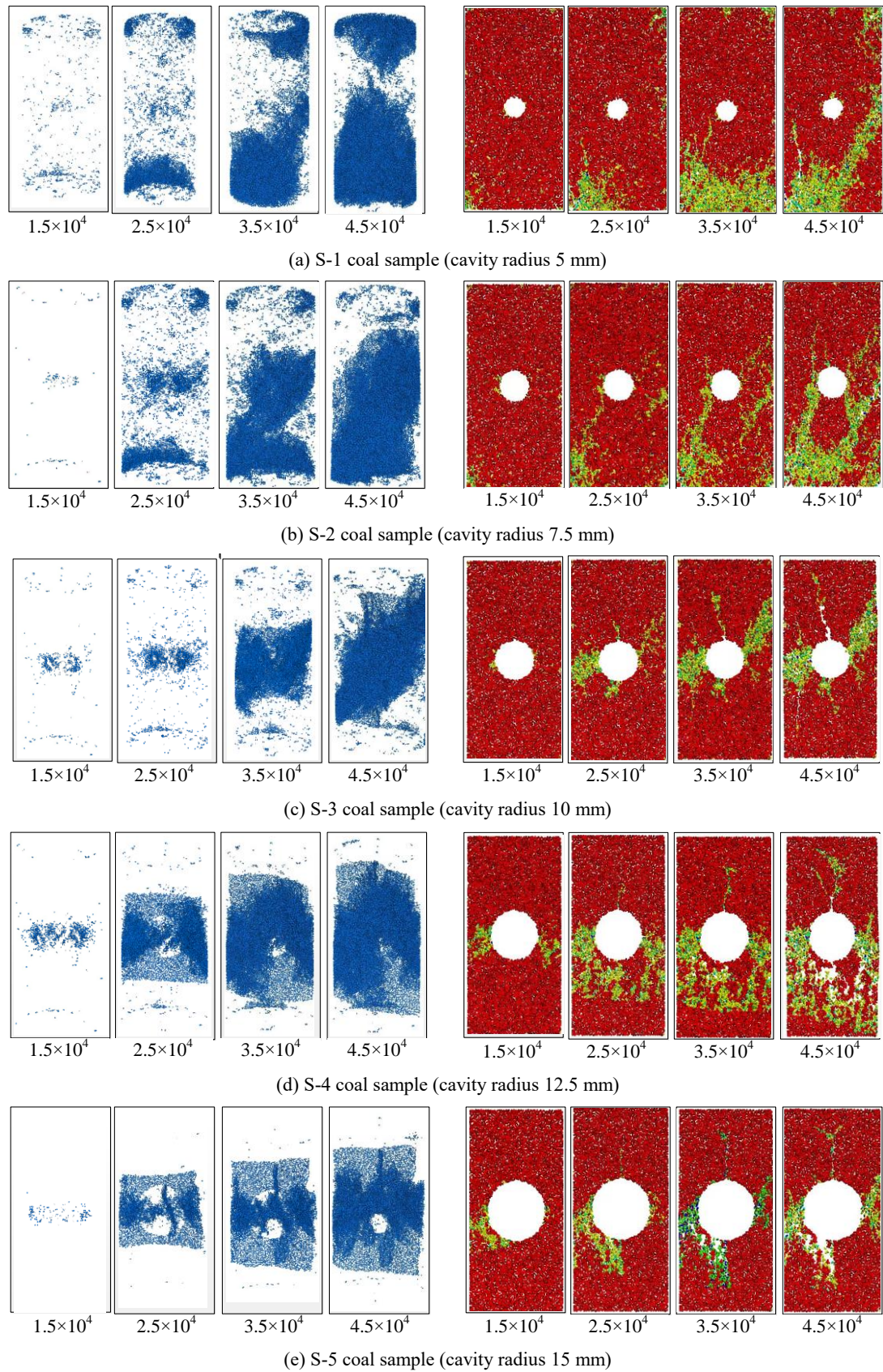


Fig. 7 Crack evolution law of coal samples with different cavity radii (Unit: Time step).

process of the specimen due to the large cavity, and more cracks were generated. The cracks of the entire specimen developed from around the cavity and expanded downward until the specimen lost stability and fails. There were only 1 to 2 cracks generated above the cavity, which was not the main factor for the failure of the sample.

For the S-5 coal sample with a cavity radius of 15 mm, cracks first germinated at the lower left of the cavity. As the loading continues, the crack area at the lower left continued to expand. At the same time, cracks began to germinate at the upper right of the cavity. Under the action of these two kinds of cracks, the cavity was damaged, driving the overall failure of the sample. In other words, the overall failure of the sample is the failure of the cavity.

5.2. CRACK EVOLUTION LAW OF COAL SAMPLES WITH DIFFERENT CAVITY SHAPES

Figure 8 shows the micro-crack evolution process of five different coal samples with cavity shapes. The left part of the figure represents the crack evolution process of different coal samples with cavity shapes, and the right part represents the bond fracture process of different coal samples with cavity shapes.

For the P-1 coal sample with a cylindrical cavity, cracks first appeared around the cylindrical cavity. At this time, the damage developed simultaneously at the upper end face, around the cavity, and the lower end face of the specimen. As the loading continues, many cracks quickly appeared in the lower half of the specimen and around the cavity. Eventually, the entire specimen was completely destroyed. From a macroscopic perspective, the cracks were mainly concentrated in the lower half of the specimen. As can be evidenced by the section shear band picture, stress concentration first occurred around the cavity, then more bonding bonds break in the lower half, and finally a shear band developed from the lower left to the upper right.

For the P-2 coal sample with a cubic cavity, the macroscopic evolution characteristics of cracks were roughly the same as those of the P-1 coal sample. Compared with the P-1 sample, the cracks of the specimen developed more evenly and the formed failure zone was more complete. From the sectional view, the lower left corner, upper right corner of the specimen and the upper right part of the cavity were stress concentration areas. The shear band first developed from the lower left corner until it was connected with the lower broken zone. At the same time, the fracture zone at the upper right corner of the specimen developed and expanded to the lower left. Eventually, it developed and penetrated downward, and the specimen was completely destroyed.

For the P-3 coal sample with a cuboid cavity, there is a big difference in the crack evolution law between the rectangular cavity specimen and the cuboid cavity specimen. Cracks first developed around the cavity and gradually expanded in all directions of the cavity, and finally were distributed throughout the entire specimen. Judging from the

shear band around the cavity, stress concentration occurred at all four corners of the rectangular cavity. The shear band first extended outward from the four corners. A shear band was quickly formed around the rectangular cavity until the specimen was completely destroyed.

For the P-4 coal sample with a trapezoidal column cavity, the crack evolution law was similar to that of the P-3 specimen when the central cavity is trapezoidal. However, the stress concentration degree at the lower left corner of the trapezoid was stronger, and the shear band was more obvious. Meanwhile, the shear band range in the upper left part was larger.

For the P-5 coal sample with a triangular prism cavity, microcracks first developed around the triangular prism cavity. Then microcracks also began to develop on the lower end face of the specimen. At the same time, the cracks expanded and penetrated, forming a fracture zone on the lower left side of the specimen. From the sectional view, the shear band first developed from the tips of the lower two corners of the triangle and developed simultaneously downward to the bottom of the specimen. Then the cracks at the tip of the upper corner of the triangle began to develop and extended to the middle and upper part of the specimen and end. Eventually, an inverted 'V'-shaped fracture zone was formed.

6. DAMAGE CONSTITUTIVE EQUATION AND VERIFICATION OF COAL SAMPLES WITH CAVITIES

6.1. ESTABLISHMENT OF DAMAGE CONSTITUTIVE EQUATION

Rock strength is a random variable affected by a combination of multiple factors. Loading damage is mainly caused by the damage of microelements inside coal during loading. These different factors are independent of each other and have a certain statistical law. Therefore, rock strength can be described by statistical distribution laws.

The microelement failure also satisfies the strength criterion and can be expressed as:

$$f(\sigma^*) - K_0 = S - K_0 = 0 \quad (1)$$

where, S , $f(\sigma^*)$ — the function of effective stress;

K_0 — coal sample strength.

When the effective stress exceeds the strength of the coal sample, the coal sample will undergo unstable failure.

Coal-rock is a heterogeneous material. The damaged micro-units are randomly distributed within the loading interval. The accumulated failed units are the integral of the random distribution function, that is:

$$N_d = \int_0^S N_t P(x) dx = N_t \int_0^S P(x) dx \quad (2)$$

where, x — distribution variable; $P(x)$ is a probability density function.

Therefore, the damage variable D during the loading process can be expressed as:

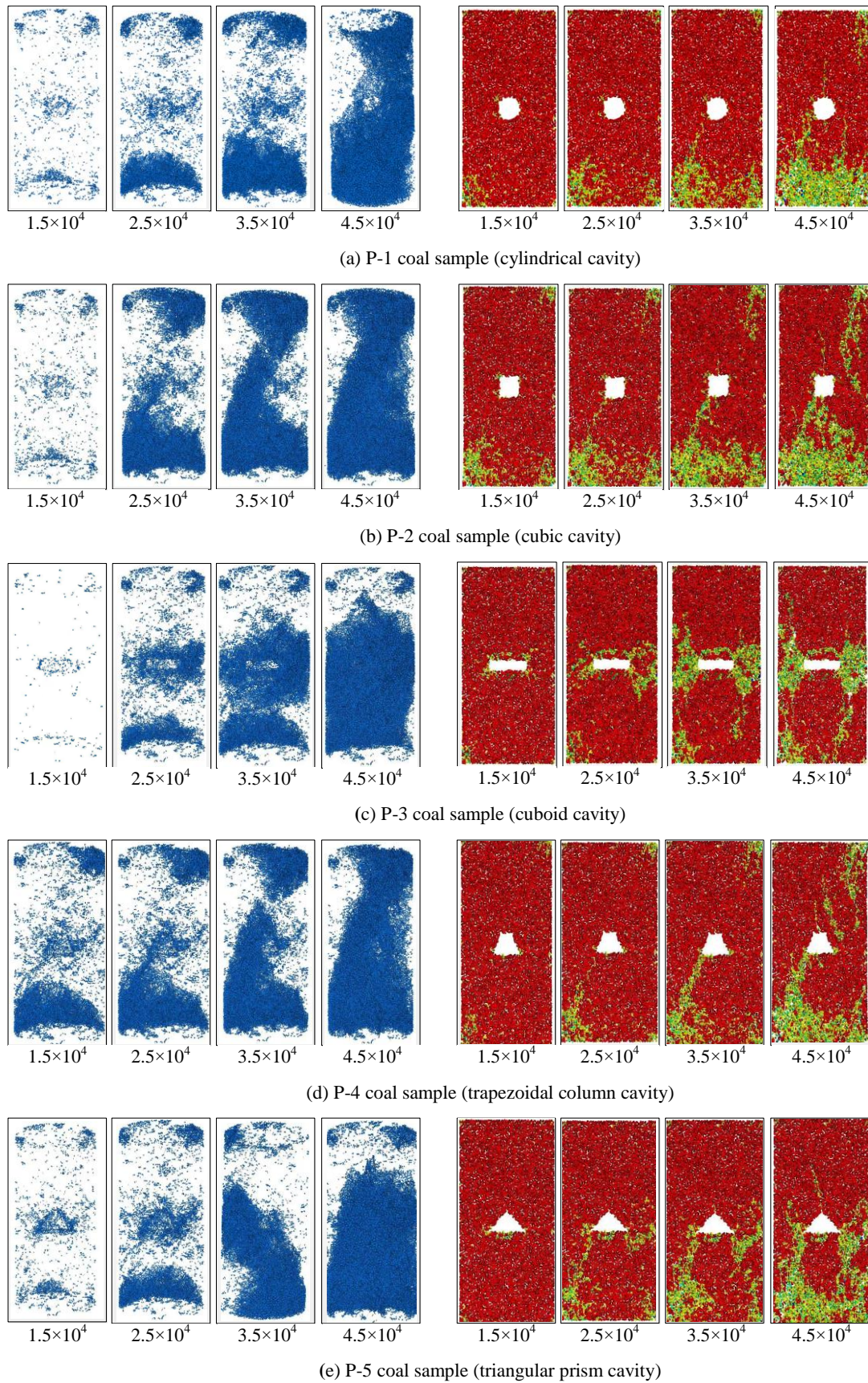


Fig. 8 Crack evolution law of coal samples with different cavity shapes.

$$D = \frac{N_d}{N_t} = \int_0^S P(x) dx \quad (3)$$

where, N_d – The number of microelements damage during the compression process;

N_t – The total number of microelements destroyed.

Assuming that the probability of strength failure of coal during compression satisfies the Weibull distribution function, $P(x)$ is expressed as:

$$P(x) = \frac{m}{S_0} \left(\frac{x}{S_0}\right)^{m-1} \exp\left[-\left(\frac{x}{S_0}\right)^m\right] \quad (4)$$

where, m , S_0 – The two parameters in the Weibull distribution function represent the density and strength of damaged microelements.

Combining Equation (3) and Equation (4), the relationship of loading damage variable D can be obtained:

$$D = 1 - \exp\left[-\left(\frac{S}{S_0}\right)^m\right] \quad (5)$$

In the above formula, the microelement strength distribution variable S can be determined by the strength criterion. In the strength criterion, the D-P strength criterion can better describe the distribution variable of coal and rock materials, and then obtain the two parameters m and S_0 .

The coal sample failure experiment under uniaxial loading mode is adopted in this paper. The expression of D-P criterion under uniaxial loading condition is:

$$\begin{cases} S - K_0 = a_0 I_1 + \sqrt{J_2} - k = 0 \\ I_1 = \sigma_1^* \\ J_2 = \frac{1}{3} \sigma_1^{*2} \end{cases} \quad (6)$$

Under uniaxial compression condition, through the strain equivalence hypothesis, the following constitutive relationship can be obtained:

$$\sigma_1 = E \varepsilon_1 (1 - D) \quad (7)$$

σ_1 and ε_1 are axial stress and axial strain. The following relationship can be obtained:

$$\begin{cases} I_1 = E \varepsilon_1 \\ \sqrt{J_2} = \frac{1}{\sqrt{3}} E \varepsilon_1 \end{cases} \quad (8)$$

According to Equation (8), by substituting the micro-element strength distribution variable S , the coal damage variable and damage equation under axial load can be obtained:

$$\begin{cases} D = 1 - \exp\left[-E^m \left(\frac{\varepsilon_1}{S_0}\right)^m \left(\alpha_0 + \frac{1}{\sqrt{3}}\right)^m\right] \\ \sigma_1 = E \varepsilon_1 \exp\left[-E^m \left(\frac{\varepsilon_1}{S_0}\right)^m \left(\alpha_0 + \frac{1}{\sqrt{3}}\right)^m\right] \end{cases} \quad (9)$$

According to the stress-strain curve, the derivative at the peak point $(\varepsilon_c, \sigma_c)$ is 0. By taking the derivative of the coal damage equation:

$$\frac{d\sigma_1}{d\varepsilon_1} = E \exp\left[-\left(\frac{S}{S_0}\right)^m\right] \left(1 - \frac{mS^{m-1}}{S_0} \left(\alpha_0 + \frac{1}{\sqrt{3}}\right) E \varepsilon_1\right) \quad (10)$$

The micro-element distribution variable S_c at the peak point can be expressed as:

$$S_c = \left(\alpha_0 + \frac{1}{\sqrt{3}}\right) E \varepsilon_c \quad (11)$$

The stress-strain relationship at the peak point can be expressed as:

$$\sigma_c = E \varepsilon_c \exp\left[-\left(\frac{S_c}{S_0}\right)^m\right] \quad (12)$$

Substituting Equation (12) into Equation (10), the values of m and S_0 can be obtained as:

$$\begin{cases} m = \frac{1}{\ln\left(\frac{E \varepsilon_c}{\sigma_c}\right)} \\ S_0 = S_c m^{\frac{1}{m}} \end{cases} \quad (13)$$

6.2. RATIONALITY VERIFICATION

6.2.1. RATIONALITY VERIFICATION OF DAMAGE CONSTITUTIVE EQUATION FOR COAL SAMPLES WITH DIFFERENT CAVITY RADII.

The elastic modulus E of intact coal samples, the compressive strength and peak strain of coal samples with different cavity radii were brought into Equation (13). The values of m and S_0 of coal sample with different cavity radii based on Weibull distribution during the damage process are shown in Table 3.

The calculated values were brought into Equation (10) to obtain the estimated values of the peak compressive strength of coal samples with different cavity radii, and were compared with the numerical simulation test values, as shown in Table 4. According to the data in Table 4, Figure 9 was plotted. As can be seen from the Figure 9, the errors between the estimated values calculated according to the damage evolution model and the test values at different cavity radii and different stages were all between 1.1 % and 9.6 %. Thus, it can be known that the constructed damage evolution equation can accurately reflect the stress-strain relationship of coal samples with different cavity radii.

6.2.2. VERIFICATION OF DAMAGE MODELS OF COAL SAMPLES WITH DIFFERENT CAVITY SHAPES.

The elastic modulus E of the intact coal sample, the peak compressive strength and peak strain of the specimens with different cavity radii were brought into Equation (13). The values of m and S_0 based on Weibull distribution of coal bodies with different cavity radii during the damage process are shown in Table 5 below.

Table 3 Values of m and S_0 for coal samples with different cavity radii.

Parameter	Cavity radius / mm				
	5	7.5	10	12.5	15
m	7.96	13.68	68.4	24.4	3.76
S_0	18.54	16.28	12.21	10.85	12.75

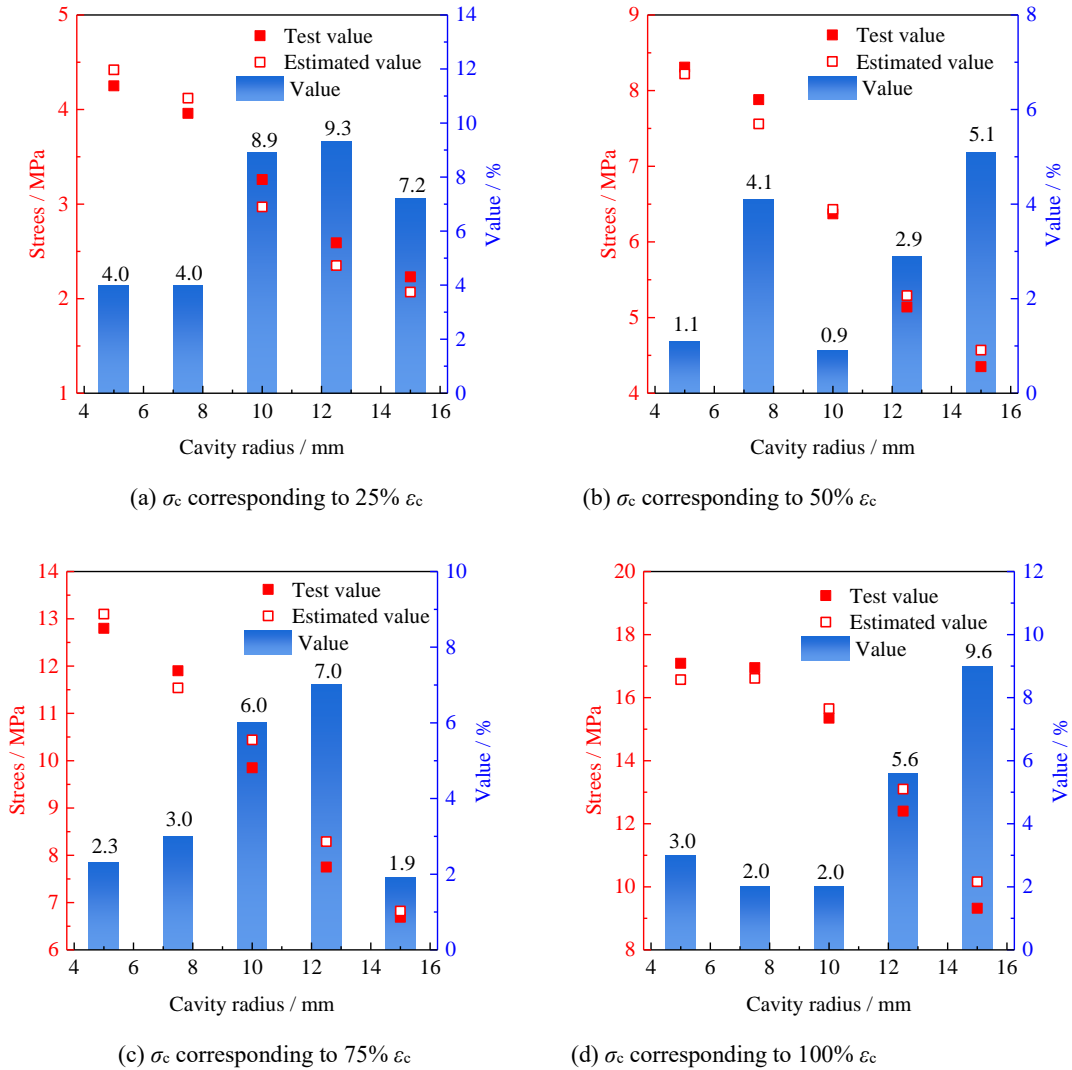


Fig. 9 Test values, estimated values and errors of axial stress of coal samples with different cavity radii at different strain stages.

The calculated values were brought into Equation (10) to obtain the estimated values of the peak compressive strength of coal samples with different cavity shapes, and were compared with the experimental values as shown in Table 6. According to the data in Table 6, Figure 10 was plotted. As can be seen from the figure, the error between the estimated value calculated according to the damage evolution model and the experimental value at different cavity shapes and different stages was between 1.0 % and 9.5 %. Thus, it can be known that the constructed damage evolution equation can accurately reflect the stress-strain relationship of coal samples with different cavity shapes.

7. ENERGY MIGRATION MODEL AND MECHANISM OF COAL SAMPLES WITH CAVITIES

A large amount of energy is accumulated inside the coal sample under the loading condition. From loading to destruction, the energy accumulated inside the coal sample not only exchanges with the outside world, but also migrates inside the coal sample (Chen et al., 2020; Chen et al., 2022; Chen et al., 2023a). The migration, accumulation and release of energy are the fundamental reasons for the instability and failure of coal samples.

To investigate the energy migration mechanism of coal samples with cavities under uniaxial

Table 4 Test values and estimated values of axial stress of coal samples with different cavity radii at different strain stages.

Cavity radius / mm	σ_c corresponding to 25 % ϵ_c / MPa			σ_c corresponding to 50 % ϵ_c / MPa			σ_c corresponding to 75 % ϵ_c / MPa			σ_c corresponding to 100 % ϵ_c / MPa		
	Test value	Estimated value	Error %	Test value	Estimated value	Error %	Test value	Estimated value	Error %	Test value	Estimated value	Error %
	5	4.25	4.42	4.0	8.31	8.22	1.1	12.8	13.1	2.3	17.09	16.57
7.5	3.96	4.12	4.0	7.88	7.56	4.1	11.9	11.54	3.0	16.95	16.61	2.0
10	3.26	2.97	8.9	6.37	6.43	0.9	9.85	10.44	6.0	15.35	15.65	2.0
12.5	2.59	2.35	9.3	5.14	5.29	2.9	7.75	8.29	7.0	12.40	13.10	5.6
15	2.23	2.07	7.2	4.35	4.57	5.1	6.69	6.82	1.9	9.32	10.16	9.0

Table 5 Values of m and S_0 for coal samples with different cavity shapes.

Parameter	Cavity shape				
	Cylinder	Cube	Cuboid	Trapezoidal column	Triangle
m	5.39	4.99	4.77	5.15	4.47
S_0	20.29	20.49	20.99	20.02	20.75

Table 6 Test values and estimated values of axial stress of coal samples with different cavity shapes at different strain stages.

Cavity shape	σ_c corresponding to 25 % ϵ_c /MPa			σ_c corresponding to 50 % ϵ_c /MPa			σ_c corresponding to 75 % ϵ_c /MPa			σ_c corresponding to 100 % ϵ_c /MPa		
	Test value	Estimated value	Error %	Test value	Estimated value	Error %	Test value	Estimated value	Error %	Test value	Estimated value	Error %
	Circular	4.33	4.42	2.1	8.64	9.16	6.0	12.9	14.1	9.3	16.7	16.19
Square	4.29	3.99	7.0	8.55	8.2	4.1	12.8	14.02	9.5	16.5	15.67	5.0
Rectangular	4.20	4.53	7.9	8.39	7.65	8.8	12.6	13.23	5.0	16.2	16.03	1.0
Trapezoidal	4.21	3.83	9.0	8.41	8.74	3.9	12.6	12.47	1.0	16.2	14.86	8.3
Triangle	4.16	3.95	5.0	8.32	8.65	4.0	12.4	12.12	2.3	16.0	16.16	1.0

compression, an energy migration model from loading to failure was constructed, as shown in Figure 11. At the outset, a small amount of energy of coal sample with cavities accumulated inside the specimen under the initial loading conditions, and the energy distribution was relatively uniform, as shown in Figure 11(a). Subsequently, as the testing machine continues to load, the energy accumulated inside the specimen gradually increases, and a large amount of energy moved to the vicinity of the cavities, accumulating near the cavities and forming stress concentration areas, as shown in Figure 11(b). Afterwards, with the continuous loading of the testing machine, the stress concentration areas near the cavities continued to accumulate energy, and when the accumulated energy reaches a certain level, new cracks and fissures were initiated inside the specimen, and the cavities also underwent deformation at the same time. The accumulated energy was dissipated in the form of internal deformation and micro-damage, as shown in Figure 11(c). Later on, As the testing machine continues to load, these deformations and micro-damages became more pronounced, the deformation of the cavities became more severe, and the number of fissures increased, as shown in Figure 11(d). Ultimately, under the loading of the testing machine, these cracks and fissures interconnect, forming large macroscopic cracks and

fissures (Chen et al., 2023b; Lai et al., 2024; Si et al., 2024; Chen et al., 2024). Additionally, as energy continuously accumulates to reach the energy storage limit of the specimen, the coal sample suddenly failed, and many fragments were ejected by the energy. Meanwhile, the energy accumulated within the coal sample was released instantaneously in the form of kinetic energy of the broken fragments, causing overall instability and destruction of the specimen.

To compare the energy transfer mechanisms between coal samples with cavities and those without, an energy transfer model for cavity-free coal samples was established, as illustrated in Figure 12. The cavity-free coal sample undergoes five stages from initial loading to final failure. In the early loading stage, the sample is mainly characterized by the closure of primary microcracks. Energy accumulates in an even and scattered manner, distributing uniformly throughout the sample (Fig. 12(a)). With continued loading, small cracks initiate within the sample, and energy begins to concentrate near the tips of these small cracks, while only a small amount of energy accumulates in crack-free regions (Fig. 12(b)). As the testing machine applies further loading, the sample continues to accumulate energy. Once the energy storage limit at the crack tips is reached, the cracks start to propagate along the tips, forming new large cracks, and energy re-concentrates at the tips of these

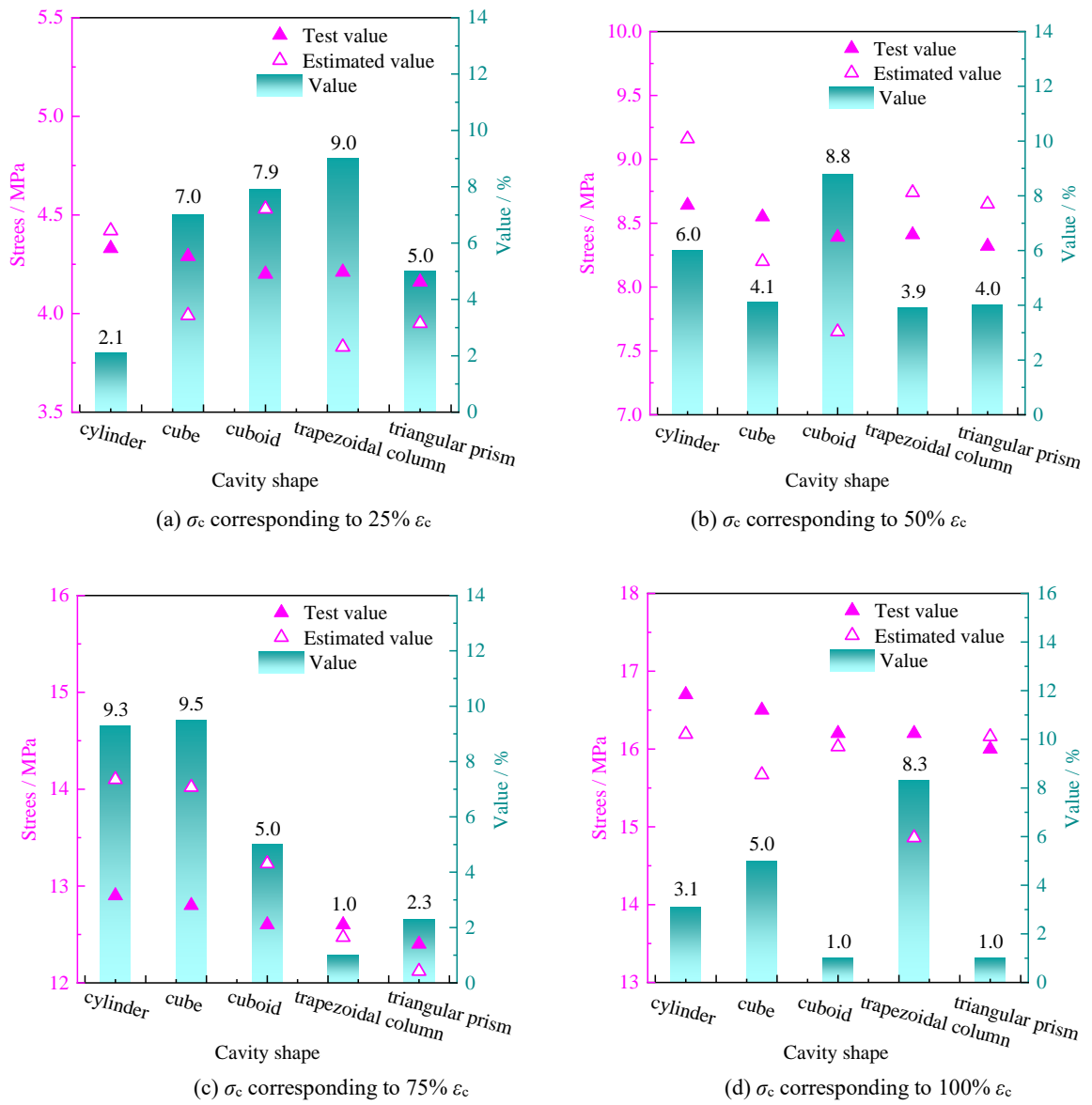


Fig. 10 Test values, estimated values and errors of axial stress of coal bodies with different cavity shapes at different strain stages.

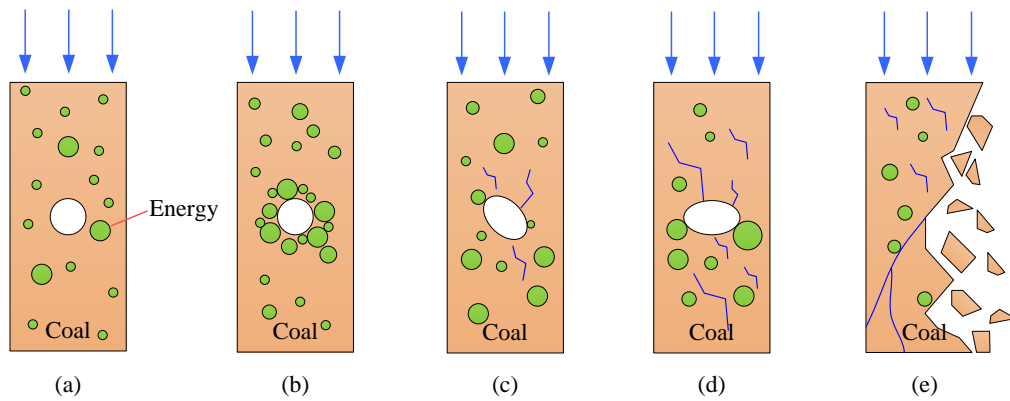


Fig. 11 Energy migration model of coal samples with cavities.

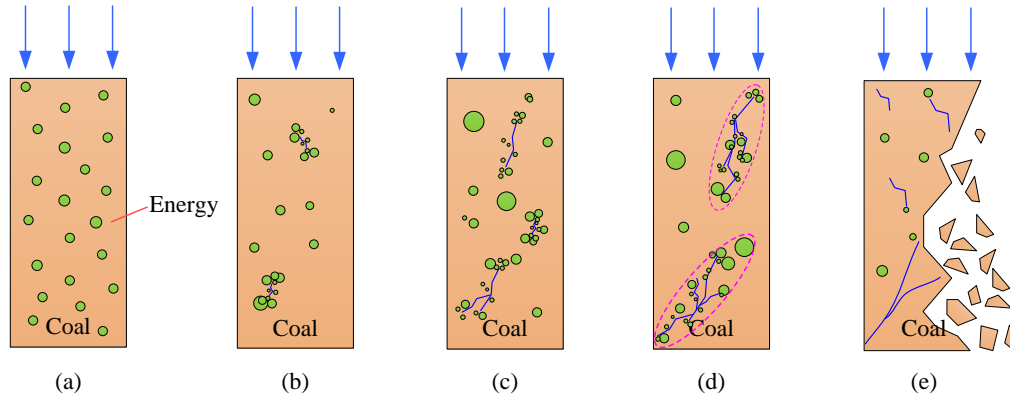


Fig. 12 Energy transfer model of cavity-free coal samples.

new cracks. Meanwhile, additional microcracks initiate at this stage, with a small portion of energy accumulating at their tips (Fig. 12(c)). Under sustained loading from the testing machine, two or more adjacent cracks interconnect, forming one or more damage zones inside the sample. Energy is mainly concentrated in these damage zones, with minimal free energy present (Fig. 12(d)). When the loading reaches the sample's energy storage limit, the larger damage zone (or a combination of several damage zones) dominates the sample's failure. Cracks within the damage zones fully develop and interconnect, leading to fragment detachment and macroscopic unstable failure of the sample. The development and interconnection of cracks in the damage zones, as well as the movement of fragments, consume a substantial amount of energy, resulting in almost no energy accumulation inside the sample at this stage (Fig. 12(e)).

In summary, the energy transfer paths and mechanisms of coal samples with cavities are entirely different from those of cavity-free samples. This is attributed to the presence of internal cavities: as a type of defect, cavities create weak zones in their vicinity, where energy tends to concentrate under loading. In contrast, cavity-free coal samples have no obvious inherent defects; defects only emerge under external loading, and these defect zones then become the main regions for energy accumulation.

8. DISCUSSION

8.1. DISCUSSION ON SAMPLE SELECTION

Coal is a kind of porous medium material containing various defects and is softer than rock (Song et al., 2023). These defects in coal greatly weaken the mechanical properties of the coal mass, making it prone to deformation and destruction. The coal mass exhibits extreme instability, which severely affects the safety and stability of underground coal-rock systems. Considering the internal structure of the coal mass, studying the mechanical properties and instability mechanisms of defective coal masses is of great theoretical significance for maintaining the

safety and stability of coal-rock systems. Therefore, mechanical numerical experiments were conducted on coal samples with different cavity radii and different shapes, and analyzed their compressive strength, elastic modulus, and other mechanical properties. The study also investigated the acoustic characteristics during the loading process, and explored the evolution of cracks to reveal the instability and destruction mechanisms. The damage constitutive model of coal sample with cavities was constructed as well. This research has achieved certain results.

However, the types of cavities are not only the five types studied in this paper, but also more irregular shapes. In addition, the cavities are not only in the center of the coal body, but also irregularly distributed in the coal body. Besides, apart from cavities, the coal mass also contains fractures as a type of defect., there are also cracks in the coal body, which is also a factor affecting the mechanical properties of the coal body. The above situations are the focus of our next research. At present, the two doctoral students under the guidance of the author are carrying out corresponding research. Due to space limitations, these research results will be presented in another article.

It is worth affirming that the research on the mechanical response and instability mechanism of coal samples with cavities carried out by the author has good reference value and theoretical significance for maintaining the safety and stability of coal-rock system.

8.2. DISCUSSION ON DAMAGE CONSTITUTIVE EQUATION

Based on the statistical distribution theory and the D-P strength criterion, the damage constitutive equation of the coal sample with cavities is constructed. The acquisition of m and S_0 parameters is based on the test in this paper. What's more, the verification results show that the damage constitutive equation has good rationality and scientificity, which provides a theoretical reference for exploring stress, strain and correlation. This is also one of the innovations of this paper.

However, in engineering practice, the defects inside the coal body are not ideal circular defects or other shape defects, mostly the combination of irregular defects and large and small cracks. The rationality of the constitutive equation under this condition needs to be further verified. In addition, the research object of this paper is coal, and the question of whether the rock material is established needs to be further verified.

It is worth affirming that the ideas and methods of constructing the damage constitutive equation are accurate and reasonable, and have high reference value for the construction of the damage constitutive equation under other defect conditions, such as the number of cavities, location, crack and other damage constitutive equations.

9. CONCLUSION

(1) The cavity radius has a great influence on the mechanical properties of coal samples. With the increase of cavity radius, the compressive strength, elastic modulus, pre-peak strain energy and impact energy index of coal samples decrease continuously. Triangular cavities have the greatest influence on the mechanical properties of coal samples, and cylindrical cavities have the least influence on coal samples.

(2) As the cavity radius increases, the peak ringing count gradually decreases, the initiation stress gradually reduces, and the cumulative ringing count gradually decreases. The coal sample with a triangular prism cavity has the highest peak ringing count and the lowest initiation stress.

(3) The crack evolution law under the influence of different cavity radii and different cavity shapes was analyzed. The larger the cavity radius, the greater the influence on the crack. In addition, with the increase of the cavity radius, the crack gradually initiates near the cavity and dominates the failure of the sample.

(4) Based on the statistical distribution theory and the D-P strength criterion, the damage constitutive equation of the coal sample with cavities is constructed and the rationality is verified. The verification error of the rationality of the damage constitutive equation of coal samples with different cavity radii is 1.1 % ~ 9.6 %, and the verification error of the damage model of coal with different cavity shapes is 1.0 % ~ 9.5 %. The accuracy of the calculation of the damage constitutive equation is more than 90 %, which can accurately reflect the stress-strain relationship of the coal sample with cavities.

(5) The energy migration model of instability and failure of coal samples with cavities is constructed. The energy migration, accumulation and release of coal samples with cavities under loading conditions are analyzed, and the instability mechanism of coal samples with cavities is clarified. Under the initial loading condition of the coal samples with cavities, a small amount of energy accumulates inside the sample, and the energy distribution is more

uniform. With the continuous loading of the testing machine, the energy accumulated inside the sample gradually increases, and a large amount of energy migrates to the cavity attachment, resulting in forming a stress concentration area near the cavity. When the accumulated energy reaches a certain degree, the cavity deforms, and new cracks and fissures are initiated inside the sample. These cracks and fissures gradually penetrate each other, and large cracks and fissures are formed macroscopically, resulting in the overall instability and failure of the sample.

FUNDING

This research was funded by National Natural Science Foundation of China (No. 52304142, 52064042, 52464014, 52464019), Natural Science Foundation of Inner Mongolia Autonomous Region of china (No. 2025YQ011, 2022MS05037), Fundamental Research Funds for Inner Mongolia University of Science & Technology (No. 2023QNJS108, 2024YXXS002, 2024RCTD015), Program for Young Talents of Science and Technology in Universities of Inner Mongolia Autonomous Region (No. NJYT22073).

DATA AVAILABILITY

All data used to support the findings of this study are included within the article, and there are not any restrictions on data access.

DECLARATIONS

The authors declare no competing interests.

REFERENCES

- Ge, L.: 2022, Study on mechanical properties and damage mechanism of coal and rocks with cavity defects under eccentric load. Liaoning Technical University (Doctoral Dissertation). DOI: 10.27210/d.cnki.glnju.2022.000867
- Gong, S., Zhao, Y., Zhou, L., Wang, Z., Guo, W., Yao, S. and Yang, D.: 2023, Dynamic fracture behavior of limestone specimens containing double cavities and crack under impact loading. *J. China Coal Soc.*, 48, 8, 3030–3047. DOI: 10.13225/j.cnki.jccs.2022.1171
- Huang, D., Zhu, Y., Qiao, S., Xing, D. and Wang, X.: 2023, Numerical experiments on macro-and micro-damage characteristics of red sandstone with pore-double fractures. *J. Shandong Univ. Sci. Technol., Nat. Sci.* 42, 4, 32–42. DOI: 10.16452/j.cnki.sdkjzk.2023.04.004
- Chen, G., Li, T., Yang, L., Zhang, G., Lyu, P. and Teng, P.: 2023a, Mechanical properties and damage characteristics of coal-rock combined samples under water-rock interaction. *Coal Sci. Technol.*, 51, 4, 37–46. DOI: 10.13199/j.cnki.cst.2020-1385
- Chen, G., Li, T., Zhang, G., Li, J., Liu, G., He, Y. and Li, Y.: 2023b, Determination of bursting liability of coal-rock combined body based on residual energy release rate index. *Chin. J. Rock Mech. Eng.*, 42, 6, 1366–1383. DOI: 10.13722/j.cnki.jrme.2022.0882
- Chen, G., Qin, Z., Zhang, G., Li, T. and Li, J.: 2019, Law of energy distribution before failure of a loaded coal-rock combined body. *Rock Soil Mech.*, 41, 6, 2021–2033. DOI: 10.16285/j.rsm.2019.0101

- Chen, G., Tang, W., Chen, S., Wang, E., Wang, C., Li, T. and Zhang, G.: 2025, Damage effect and deterioration mechanism of mechanical properties of fractured coal-rock combined body under water-rock interaction. *Rock Mech. Rock Eng.*, 58, 1, 513–537. DOI: 10.1007/s00603-024-04163-3
- Chen, G., Zhang, J., He, Y., Zhang, G. and Li, T.: 2022, Derivation of pre-peak energy distribution formula and energy accumulation tests of coal-rock combined body. *Rock Soil Mech.*, 43, S2, 130–143+154. DOI: 10.16285/j.rsm.2021.0704
- Lai, X., Fang, X., Shan, P., Cui, F., Chen, J., Zhang, S. and Liu, X.: 2021b, Failure mode and phased energy accumulation and release law of brittle holey coal samples during loading. *J. Min. Saf. Eng.*, 38, 5, 1005–1014. DOI: 10.13545/j.cnki.jmse.2021.0136
- Lai, X., Ren, J., Shan, P., Cui, F., Cao, J., Liu, B. and Yang, Y.: 2021a, Evolution law of characteristic energy of coal samples with different pore diameters and bursting liability. *J. Cent. South Univ.*, 52, 8, 2601–2610. DOI: 10.11817/j.issn.1672-7207.2021.08.008
- Lai, X., Xu, H., Shan, P., Hu, Q., Ding, W., Yang, S. and Yan, Z.: 2024, Research on the mechanism of rock-burst induced by mined coal-rock linkage of sharply inclined coal seams. *Int. J. Miner. Metall. Mater.*, 31, 5, 929–942. DOI: 10.1007/s12613-024-2833-8
- Li, D., Cheng, T., Zhou, T. and Li, X.: 2015, Experimental study of the dynamic strength and fracturing characteristics of marble specimens with a single cavity under impact loading. *Chin. J. Rock Mech. Eng.*, 34, 2, 249–260. DOI: 10.13722/j.cnki.jrme.2015.02.004
- Li, L., Tang, L., Pan, Y., Ju, X. and Sun, Y.: 2022, Experimental study of anomalously low friction effect of porous block under stress wave disturbance. *Chin. J. Undergr. Space Eng.*, 18, 5, 1605–1614. DOI: 10.20174/j.juse.2022.05.022
- Liu, G., Wang, D. and Yang, Z.: 2023, Mechanical properties and acoustic emission characteristics behind three-holes sandstone under bias loading. *J. Heilongjiang Univ. Sci. Technol.*, 33, 6, 875–881. DOI: 10.3969/j.issn.2095-7262.2023.06.016
- Liu, P., Liu, Q., Xia, M., Luo, Y., Chen, Z., Huang, X. and Bo, Y.: 2024, Effect of hole shapes on mechanical behavior of layered rocks using FDEM numerical method. *J. Cent. South Univ.*, 55, 2, 595–606. DOI: 10.11817/j.issn.1672-7207.2024.02.013
- Liu, X.: 2022, Quantitative investigation on the mechanical characteristics and cracking behavior of rock masses containing an opening and joints. Kunming University of Science and Technology (Doctoral Dissertation). DOI: 10.27200/d.cnki.gkmlu.2022.000023
- Pan, Y., Dai, L., Li, G. and Li, Z.: 2021, Study on compound disaster of rock burst and roof falling in coal mines. *J. China Coal Soc.*, 46, 1, 112–122. DOI: 10.13225/j.cnki.jccs.2020.0557
- Pi, Z., Zhou, Z., Wang, S., Jing, Y. and Cai, X.: 2023, Failure characteristics of cuboid sandstone with D-shaped cavity under biaxial loading and unloading conditions. *J. Cent. South Univ.*, 54, 8, 3154–3167. DOI: 10.11817/j.issn.1672-7207.2023.08.019
- Qi, Q., Pan, Y., Li, H., Jiang, D., Shu, L., Zhao, S., Zhang, Y., Pan, J., Li, H. and Pan, P.: 2020, Theoretical basis and key technology of prevention and control of coal-rock dynamic disasters in deep coal mining. *J. China Coal Soc.*, 45, 5, 1567–1584. DOI: 10.13225/j.cnki.jccs.DY20.0453
- Si, X., Luo, Y. and Luo, S.: 2024, Influence of lithology and bedding orientation on failure behavior of “D” shaped tunnel. *Theor. Appl. Fract. Mech.*, 129: 104219. DOI: 10.1016/j.tafmec.2023.104219
- Song, Z., Zhang, J., Zhang, Y., Dong, X. and Wang, S.: 2023, Characterization and evaluation of brittleness of deep bedded sandstone from the perspective of the whole life-cycle evolution process. *Int. J. Min. Sci. Technol.*, 33, 4, 481–502. DOI: 10.1016/j.ijmst.2022.12.007
- Wang, T., Ge, L., Zhao, H., Zhang, X., Zhang, H. and Li, W.: 2022, Deformation damage characteristics and constitutive model of raw coal and briquette with central cavity under asymmetric loading. *J. China Coal Soc.*, 47, 11, 4040–4054. DOI: 10.13225/j.cnki.jccs.2021.1933
- Wang, X., Zhao, Y., Feng, Y., Wang, Z., Li, Y., Chen, B., Dong, Z. and Wu, S.: 2024, Simulation of cracks propagation and fractal characteristics of composite rock strata with cavities and fractures. *Saf. Coal Mines.*, 55, 1, 42–49. DOI: 10.13347/j.cnki.mkaq.20221467
- Wang, Y., Zhang, Y., Nie, J. and Liu, J.: 2023, Mechanical properties of sandstone with cavities under impact load. *J. Min. Strat. Control Eng.*, 5, 1, 013024. DOI: 10.13532/j.jmsce.cn10-1638/td.20221212.001
- Wu, H., Fan, A., Jia, Y., Wang, M., Li, S. and Zhang, B.: 2023, Mechanical properties and fracture mechanism of pre-holed rock under impact load. *Blasting*, 40, 4, 1–12. DOI: 10.3963/j.issn.1001-487X.2023.04.001
- Xiao, F., Meng, X., Bashkov, O.V., Bao, F., Liu, L. and Xing, L.: 2022, Experimental study on effect of artificial defects on coal sample damage with different diameter holes. *J. Heilongjiang Univ. Sci. Technol.*, 32, 3, 269–274. DOI: 10.3969/j.issn.2095-7262.2022.03.001
- Yang, S., Liu, X. and Li, Y.: 2012, Experimental analysis of mechanical behavior of sandstone containing cavity and fissure under uniaxial compression. *Chin. J. Rock Mech. Eng.*, 31, S2, 3539–3546. <https://rockmech.whrsm.ac.cn/CN/Y2012/V31/Is2/3539>
- Yuan, L.: 2021, Research progress of mining response and disaster prevention and control in deep coal mines. *J. China Coal Soc.*, 46, 3, 716–725. DOI: 10.13225/j.cnki.jccs.YT21.0158
- Zhang, T., Jing, C., Wang, X., Guo, H., Zhang, L. and Pan, H.: 2021, Experimental investigation of the effect of different loading rates on deformation characteristics of porous samples. *J. Min. Saf. Eng.*, 38, 4, 847–856. DOI: 10.13545/j.cnki.jmse.2020.0254
- Zhao, G., Wang, E., Wu, H., Qiu, J. and Dai, Y.: 2019, Micro-fracture evolution rule of sandstone specimens with a single cavity under uniaxial compression. *J. Cent. South Univ.*, 50, 8, 1891–1900. DOI: 10.11817/j.issn.1672-7207.2019.08.017
- Zhao, H., Tao, M., Li, X. and Zhao, R.: 2023, Mechanical characteristics and fracture mechanism of cylindrical cavity granite under one-dimensional coupled static-dynamic load. *Chin. J. Nonferrous Met.*, 33, 9, 3077–3091. DOI: 10.11817/j.ysxb.1004.0609.2022-43692
- Zhou, Z., Sun, J., Wang, H. and Guo, Y.: 2021, Strain evolution and failure characteristics of granite with cavities under impact load. *J. Cent. South Univ.*, 52, 3, 681–692. DOI: 10.11817/j.issn.1672-7207.2021.03.003